Torque Based Direct Driving Force Control Method with Driving Stiffness Estimation for Electric Vehicle with In-Wheel Motor

Junya Amada and Hiroshi Fujimoto
The University of Tokyo
5-1-5, Kashiwanoha, Kashiwa, Chiba, 227-8561 Japan
Phone: +81-4-7136-3881
Fax: +81-4-7136-3881
Email: amada@hflab.k.u-tokyo.ac.jp , fujimoto@k.u-tokyo.ac.jp

***Abstract*—In order to control the motion of electric vehicles (EVs), it is important to control the driving force. Author's research group had proposed the driving force control method which uses wheel speed control. However, this control method has a limitation on the achievable control bandwidth due to multiple control loops. In this paper, a new driving force control method for EVs based on driving stiffness estimation is proposed. This method can achieve direct and quick driving force control. The effectiveness of the proposed control method is verified through simulations and experiments.**

I. Introduction

Nowadays, the environmental problems such as global warming, exhaustion of fossil fuels, and air pollution are getting serious. Therefore, Electric Vehicles (EVs) have attracted a great deal of interest as zero-emission vehicle. In addition, EVs have following three advantages [1].

- Development of in-wheel motors enables individual control of each wheel.
- Generated torque can be measured precisely from motor current.
- Torque response is quick.

These advantages are effective for vehicle motion control [1]–[5]. Author's research group has studied on the vehicle motion control based on quick torque response of in wheel motors (IWM) [6]–[8].

Previous studies of vehicle motion control is based on assumption that tires adhere to road [7], assuming that all of the motor torque becomes a driving force. So, driving force control cannot be achieved when the tire is slipping on the low μ road. Moreover, even on the high μ road, we have to design the motion controller considering the wheel dynamics to strictly control the driving force.

Driving force control method [8] is one of the EV's traction control methods considering tire slip. This control method can track driving force reference even on the low μ road. If the driving force reference is too large to realize, this method achieves the maximum allowable driving force with respect to the road condition. However, this method has limitations in the control bandwidth caused by the delay in the driving force observer and multiple control loops (e.g., driving force control loop, wheel speed loop and current loop).

This paper proposes a quick driving force control method by removing inner wheel speed control loop. Driving force control on high μ road is mainly achieved by feedforward torque command calculated from the summation of driving force torque term and inertial torque compensation term. By using this feedforward controller, quick driving force response is obtained.

However, the proposed control method does not have effect on traction on the low μ road. Then in addition to this controller, the reference limitation is used together to keep adhesion of tire and road. The range of limiter is determined from estimated driving stiffness. Estimation method is based on the recursive least squares algorithm. Simulations and experiments are carried out to confirm the effectiveness of the proposed method.

II. Experimental Vehicle and Vehicle Model

A. Experimental Vehicle

An original experimental EV "FPEV2-Kanon" which is developed in the author's laboratory, is used for performance verification. In this section, the characteristics of the experimental vehicle are explained. In-wheel motors which are outer-rotor type, are installed in each wheel. Since these motors use direct drive mechanism, the reaction force from the road is directly transferred to the motor side without any adverse effects by gear reduction and backlash. The experimental vehicle is shown in Fig. 1 and its specifications are shown in Table. I.

B. Vehicle Model

The longitudinal vehicle motion dynamics is described in this section. One wheel model is shown in Fig. 2. The dynamic equations of the wheel and chassis longitudinal motion can be expressed as

$$J\dot{\omega} = T - rF_d, \tag{1}$$

$$M\dot{V} = F_d, \tag{2}$$

Fig. 1. FPEV2-Kanon.

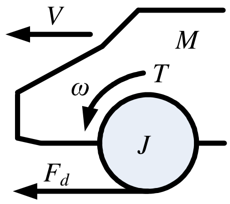

Fig. 2. One wheel vehicle model.

TABLE I
VEHICLE SPECIFICATION OF KANON.

Weight(include wheel mass) M	850 [kg]
Radius of tire r	0.302 [m]
Inertia of front wheel J	1.24 [Nms^2]
Front in-wheel motor specification	
Rated torque	110 [Nm]
Maximum torque	500 [Nm]
Rated power	6.0 [kW]
Maximum power	20.0 [kW]
Maximum speed	1113 [rpm]
Weight	32 [kg]

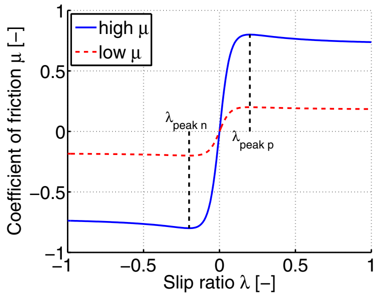

Fig. 3. μ–λ curve.

where T[Nm] is the motor torque, F_d[N] is the driving force, r[m] is the wheel radius, ω[rad/s] is the wheel angular velocity, J[Nms^2] is the wheel inertia, M[kg] is the vehicle mass and V[m/s] is the vehicle speed. In addition, F_d is represented by

$$F_d = \mu N, \tag{3}$$

where N[N] is the normal force of each wheel and μ is the friction coefficient. This friction coefficient varies with respect to the slip ratio λ which is defined as

$$\lambda = \frac{V_\omega - V}{\max(V_\omega, V, \varepsilon)}, \tag{4}$$

where V_ω is wheel speed $r\omega$, ε is a small constant to avoid zero division. It is known that the tire–road coefficient of friction has the relationship with slip ratio as shown in Fig. 3 [9]. When the slip ratio is small, the friction coefficient is nearly proportional to the slip ratio. This proportional constant D_s is driving stiffness. Driving force is calculable by the product of λ and D_s as expressed in (5). The value of a driving stiffness varies with road conditions.

$$F_d \simeq D_s \lambda. \tag{5}$$

III. DIRECT DRIVING FORCE CONTROL SYSTEM BASED ON WHEEL DYNAMICS (PROPOSED METHOD 1)

A. A Schematic of Proposed Method

In this paper, the proposed direct driving force control system is designed based on two degree of freedom control methodology. The feedforward (FF) controller is mainly used to improve the control bandwidth. The feedback (FB) controller suppresses the disturbance and a modeling error. The driving force is not measurable. Therefore, it is estimated with the driving force observer [1]. The block diagram of proposed method is shown in Fig. 4.

B. Feedforward Control

From (1), the driving force reference is achieved by the torque reference which is represented by

$$T^*_{ff} = rF^*_d + J\dot{\omega}, \tag{6}$$

where, T^*_{ff} is the motor torque reference from feedforward controller.

However, the second term on the right side of (6) $J\dot{\omega}$ increases immediately and accelerate the tire when F^*_d exceeds the realizable driving force and the tire is slipping. Then, the inertial torque $J\dot{\omega}$ is calculated using vehicle velocity as

$$\dot{\omega} = \frac{\dot{V}}{r} = \frac{a_x}{r}. \tag{7}$$

However, even if the tire slips, the vehicle velocity does not increase immediately. Therefore, compensating the inertial torque on high μ load and suppressing the sudden increase of the inertial torque on a slippery road are achieved.

C. Design of Feedback Controller

The gain of FB controller is determined by pole placement method. Here, we have developed the plant model used in pole placement. The slip ratio is defined as

$$\lambda = \frac{r\omega - V}{r\omega}. \tag{8}$$

By differentiating (8) with respect to ω, we can obtain a dynamic equation as follows :

$$\dot{\omega} \;\; = \;\; \frac{(1-\lambda)\dot{V} + \dot{\lambda}V}{r(1-\lambda)^2}. \tag{9}$$

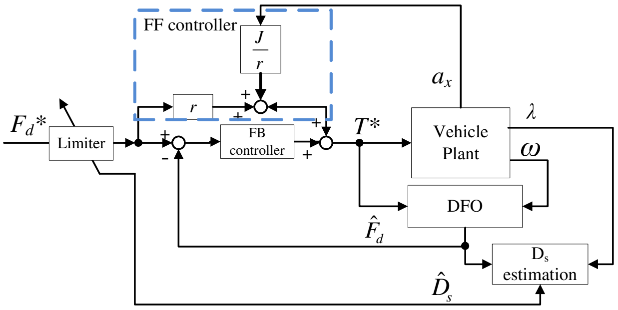

Fig. 4. Block diagram of direct driving force control.

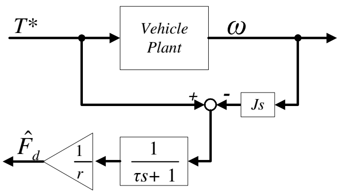

Fig. 5. Driving force observer.

By substituting (1) and (2) into (9), the following equation is obtained.

$$T = \left(r + \frac{J}{rM(1-\lambda)}\right) F_d + \frac{J\dot{\lambda}V}{r(1-\lambda)^2} \tag{10}$$

A FB controller is designed for compensating the steady-state error only. Therefore, $\dot{\lambda}$ in (10) is approximately zero and thereby (10) can be simplified as,

$$F_d = \frac{1}{r + \frac{J}{rM(1-\lambda)}} T. \tag{11}$$

By using this equation, the gain of controller can be designed. Here, the nominal slip ratio is selected as $\lambda_n = 0.01$. The plant has no integral characteristic. Therefore, I-controller is applied. Thus, the FB signal is estimated driving force by driving force observer (DFO).

D. Driving Force Observer

In (1), the motor torque is calculated from current in motor. Moreover, $\dot{\omega}$ is also calculable. Therefore, driving force can be estimated by using DFO [1] based on (12).

$$\hat{F}_d = T - J\dot{\omega} \tag{12}$$

The block diagram of DFO is shown in Fig. 5.

IV. Direct Driving Force Control System Considering Limitation of the Driving Force Refference (Proposed Method 2)

A. Traction Control Based on the Reference Limitation

The FF controller mentioned in section III constantly works to achieve F_d^*. Moreover, FB controller works to suppress the tracking error. Therefore, the controller mentioned in previous section accelerates the slipping wheel when the driving force reference exceeds the maximum driving force on the road.

Then, the proposed method 2 has a limiter on the driving force reference. When the road conditions change, the maximum value of the limiter is reduced. By using the reference limitation, wheel speed control is not required. In this paper, the range of limiter is determined by estimating driving stiffness.

The value of maximum driving force is calculated by multiplying estimated driving stiffness $\hat{D}_s$ and optimal slip ratio λ_{peak}. The range of limitation is set at the estimated maximum driving force as expressed in (13). $\hat{D}_s$ estimation algorithm will be discussed in the next section.

$$\begin{cases} F_{d\ \max} = \hat{D}_s \lambda_{\mathrm{peak\,p}}, \\ F_{d\ \min} = \hat{D}_s \lambda_{\mathrm{peak\,n}}. \end{cases} \tag{13}$$

In this paper, $\lambda_{\mathrm{peak\,p}}$ and $\lambda_{\mathrm{peak\,n}}$ are treated as known parameters and their values are 0.2 and -0.2 respectively.

B. Driving Stiffness Estimation Method

As shown in (5), the driving force is nearly proportional to the slip ratio and the proportional constant is defined as driving stiffness. Then, the value of driving stiffness can be estimated by applying the recursive least-squares algorithm (RLS) using the forgetting factor on λ and $\hat{F}_d$ [10]. When observable signal ξ and y has relation as represented (14), a RLS algorithm for θ estimation is shown in (15).

$$y = \theta \cdot \xi \tag{14}$$

$$\hat{\theta}(k) = \hat{\theta}(k-1) - \frac{\Gamma(k-1)\xi(k)}{\rho + \xi(k)\Gamma(k-1)\xi(k)} \left[\xi(k)\hat{\theta}(k-1) - y(k)\right] \tag{15}$$

where, ρ is the forgetting factor, $\Gamma(k)$ is rewritten in (16).

$$\Gamma(k) = \frac{1}{\rho}\left[\Gamma(k-1) - \frac{\Gamma(k-1)\xi^2(k)\Gamma(k-1)}{\rho + \xi(k)\Gamma(k-1)\xi(k)}\right] \tag{16}$$

Then, by substituting $\xi = \lambda$ and $y = \hat{F}_d$ in (14), $\hat{\theta} = \hat{D}_s$ can be estimated.

Here, precision of estimated value is low when signal used in RLS is small [11]. Therefore, update of driving stiffness estimation is stopped as shown in (17). That is to say, when $\xi < \varepsilon_\lambda$,

$$\begin{cases} \theta[k] = \theta[k-1] \\ \Gamma[k] = \Gamma[k-1] \end{cases} \tag{17}$$

where, ε_λ is a small value.

V. Simulation

Simulation is carried out to verify the effectiveness of the proposed methods, i.e., driving force control based on driving stiffness estimation. The vehicle parameters used in simulation are shown in Table. I. Magic Formula tire model [9] is used in this simulation. The maximum value of friction coefficient μ_{peak} is set to 0.8 on high μ road and 0.2 on low μ road. λ_{peak} is set to 0.2.

The pole value used for the pole placement of FB controller is -3 [rad/s]. The driving force reference is step signal applied first-order lag element. The amplitude of step is $450[\mathrm{N}]$. The vehicle runs on high μ road for 2 [sec], then goes to low μ road. After 4 sec from the start, vehicle goes into high μ road again.

Parameters used in D_s estimation are minute slip ratio for conditional updating $\varepsilon_\lambda = 0.01$, forgetting factor $\rho = 0.95$ and sampling time $T_s = 1[\mathrm{ms}]$. When the vehicle moves slowly, calculated slip ratio becomes significantly inaccurate. Therefore, updating of D_s estimation starts if the condition $V > 0.1$ $[\mathrm{m/s}]$ is satisfied.

Fig. 6 to 8 are simulation results. In this paper, "Without control" means that the torque command contains only driving force torque term $T^* = rF_d^*$. "Proposed method 1" is the method using $T^* = rF_d^* + J\dot{\omega}$, and "Proposed method 2" is the combination of "Proposed method 1" and the limitation for the driving force reference.

Fig. 6 is the result of "Without control". Fig. 6(d) shows the error of driving force. From this result, the estimated driving force value has errors even on the high μ road. So, strict driving force control cannot be achieved without considering inertial torque. Fig. 7 is the result of "Proposed method 1", considering inertial torque term. As shown in Fig. 7(d), the error of driving force is reduced compare to "Without control". Therefore, by considering inertial torque, driving force control by FF controller is achieved on high μ road.

However, the "Proposed method 1" does not have the ability to keep adhesion between road and tire. So, once vehicle goes into low μ road, the tire lose traction with the road. As a result, wheel speed and slip ratio increase extremely as shown in Fig. 7(b) and Fig. 7(c).

Here, the reference limiter based on D_s estimation is combined with 2-DOF controller (Proposed method 2). Then, the slip of tire is reduced as shown in Fig. 8(b) and 8(c). Moreover, the slip ratio converges on setup optimal slip ratio $\lambda_{\mathrm{peak\,p}}$ (Fig. 8(c)). Therefore, maximum driving force output is achieved by setting $\lambda_{\mathrm{peak\,p}}$ to optimal value.

VI. Experiment

In this section, the effectiveness of proposed method is verified through experiments. The vehicle runs from the high μ road and go through the low μ road. A polymer sheet is used for a slippery (low μ) road. By watering this sheet, a low μ road with approximately $\mu = 0.2$ can be realized.

In this experiment, only front wheels are drive wheels. Then, the vehicle velocity is measured by wheel speed of non-drive wheels. This vehicle velocity is used for calculating the slip ratio λ. The parameters used in D_s estimation are the same as the simulation.

Fig. 9 is the result of "Without control", Fig. 10 is the result of "Proposed method 1" and Fig. 11 is the result of "Proposed method 2". Here, plotted slip ratio value is changed to zero during $V < 0.2$ $[\mathrm{m/s}]$, because the precision of slip ratio is low during vehicle velocity is low.

Trends of the result are consistent with simulation. Comparing Fig. 9(d) and Fig. 10(d), the effect of compensation of inertial term is confirmed. In addition, comparing 10(c) and 11(c), a traction control is succesfully achieved by employing the reference limiter.

VII. Response Speed of Proposed Method

In this section, the response speed of proposed driving force control method is evaluated. On high μ road, the response speed of the proposed method is mainly affected by FF controller. Therefore, the torque reference is fixed immediately. And, on low μ road, the convergence time of D_s estimation affects on the response speed dominantly. One of the indicator of the convergence time of RLS method is the memory time constant T_0 shown in (18).

$$T_0 = \frac{1}{1-\rho}, \tag{18}$$

where ρ is the forgetting factor used in RLS. The estimation value is much influenced by the observed value T_0 sample times ago. In this paper, the sample time T_s and the forgetting factor ρ are set to $T_s = 1[\mathrm{ms}]$ and $\rho = 0.95$. Therefore, the estimation of D_s converges in 20 ms.

In fact, the result of D_s estimation shows that estimation of D_s converges within 100 [ms] after going into the low μ load. It is reasnable value considering the 40 [ms] time constant for DFO

In contrast, a conventional driving force control method, which is based on wheel speed control, has 50 [ms] of time constant for wheel speed controller and 30 [ms] of time constant for DFO. The time constant for driving force control loop should be larger than these values. Therefore, the faster response driving force control method is achievable by using proposed driving force control method.

VIII. Conclusion

In this paper, the driving force control method using 2 DOF control and the reference limiter based on D_s estimation is proposed. The effectiveness of the proposed method is confirmed by the simulation and the experiment. On the high μ load, driving force can be controlled. And, when the driving force is saturated, traction control is achieved.

The future work is to consider the λ_{peak} estimation method. In this paper λ_{peak}, the slip ratio that achieves the maximum driving force, is dealt as well-known. However, the value of λ_{peak} varies with change of load conditions. By estimating λ_{peak}, more strict driving force control will be achieved.

Acknowledgement

This research was partly supported by Industrial Technology Research Grant Program from New Energy and Industrial Technology Development Organization (NEDO) of Japan.

References

[1] Y. Hori, "Future vehicle driven by electricity and control — research on four-wheel-motored "UOT Electric March II" ",IEEE Trans. on Industrial Electronics, Vol.51, No.5, pp.954–962, 2004

[2] D. Foito, M. Guerreiro and A.Cordeiro, "Anti-slip wheel controller drive foe EV using speed and torque observers",in Proc. the 18th International Conference on Electrical Machines, pp.1–5, 2008

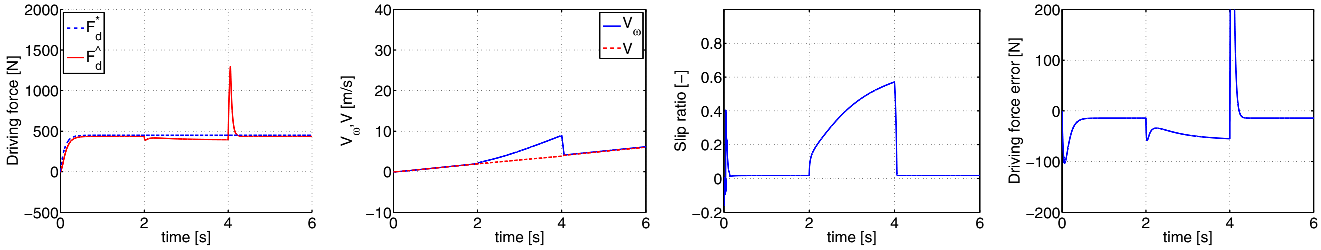

(a) Driving force. (b) Wheel velocity, Vehicle velocity. (c) Slip ratio. (d) Error of driving force.

Fig. 6. Simulation result (Without control).

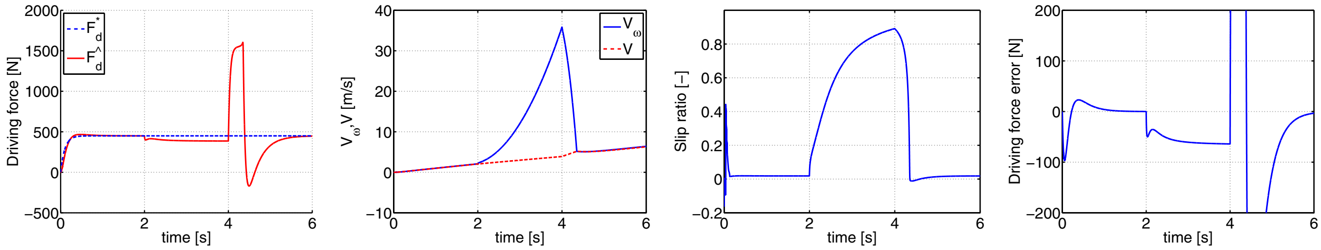

(a) Driving force. (b) Wheel velocity, Vehicle velocity. (c) Slip ratio. (d) Error of driving force.

Fig. 7. Simulation result (Proposed method 1).

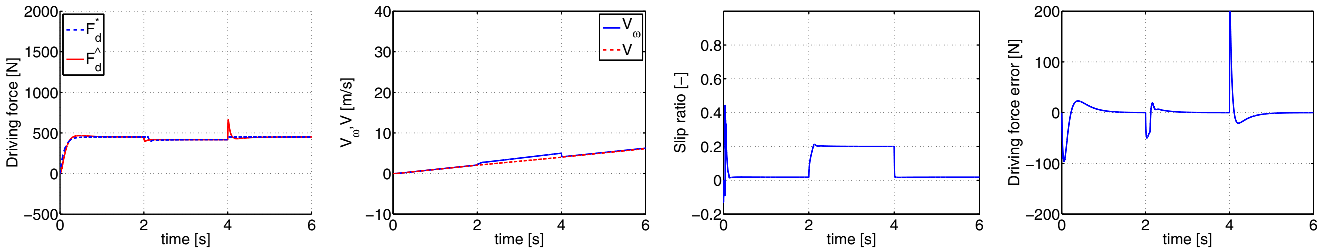

(a) Driving force. (b) Wheel velocity, Vehicle velocity. (c) Slip ratio. (d) Error of driving force.

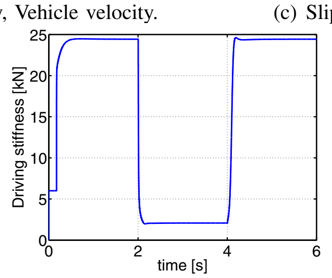

(e) Driving stiffness.

Fig. 8. Simulation result (Proposed method 2).

[3] Yinghui Ge and C.S. Chang, "Torque distribution control for electric vehicle based on traction force observer", in Proc. the IEEE International Conference on Computer Science and Automation Engineering, pp.371–375, 2011

[4] H. Ogura and T. Murakammi, "Improvement of vehicle stability by reaction force control on accelerator pedal and steering wheel", in Proc. International Power Electronics Conference, pp.2956–2963, 2010

[5] N. Mutoh and H. Akashi, "Electric and mechanical brake cooperative control method for FRID EVs under various severe road conditions ", in Proc. 37th Annual Conference of the IEEE Industrial Electronics Society, Melbourne, Australia, pp.4570 – 4576 , 2011

[6] H. Fujimoto, "Regenerative Brake and Slip Angle Control of Electric Vehicle with In-wheel Motor and Active Front Steering" , in Proc. , Yokohama, Japan, pp.1–7, 2011.

[7] S. Egami, H. Fujimoto, "Range Extension Control System for Electric Vehicles Based on Front and Rear Driving Force Distribution Considering Load Transfer", in Proc. The 37th Annual Conference of the IEEE Industrial Electronics Society, Melbourne, Australia, pp.3721-3726, 2011.

[8] K. Maeda, H. Fujimoto and Y. Hori, "Four-wheel Driving-force Distribution method for Instantaneous or Split Slippery Roads for Electric Vehicle with In-wheel Motors", Trans. The 12th International Workshop on Advanced Motion Control, No.50, pp.1–6, 2012

[9] H.B.Pacejka and E.Bakker, "The Magic Formula Tyre Model", Tyre models for vehicle dynamic analysis: proceedings of the 1st International Colloquium on Tyre Models for Vehicle Dynamics Analysis, held in Delft, The Netherlands, 1991

[10] T. Kanou and H. Fujimoto, "Slip-ratio Based Yaw-rate Control with Driving Stiffness Identification for Electric Vehicle", 9th International Symposium on Advanced Vehicle Control, Japan, pp. 786–791, 2008

[11] H. Fujimoto and B. Yao, "Multirate Adaptive Robust Control for Discrete-time Non-minimum Phase Systems and Application to Linear Motors", IEEE/ASME Trans. Mechatronics, vol.10, no.4, pp.371–377, 2005

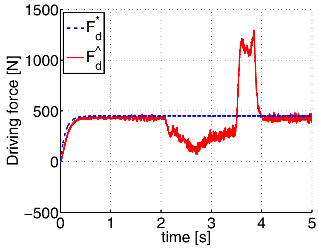

(a) Driving force.

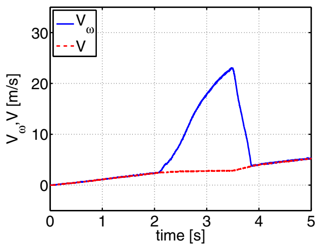

(b) Wheel velocity, Vehicle velocity.

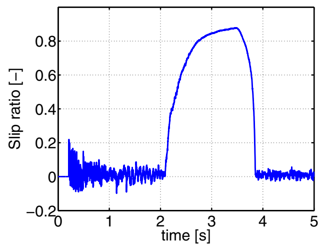

(c) Slip ratio.

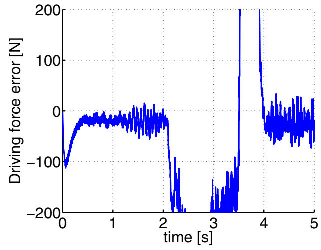

(d) Error of driving force.

Fig. 9. Experimental Result (Without control).

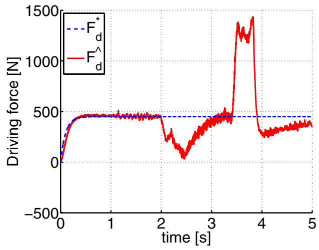

(a) Driving force.

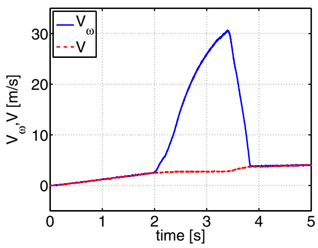

(b) Wheel velocity, Vehicle velocity.

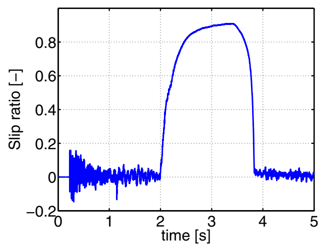

(c) Slip ratio.

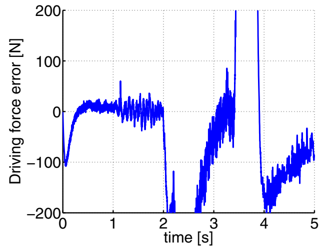

(d) Error of driving force.

Fig. 10. Experimental Result (Proposed method 1).

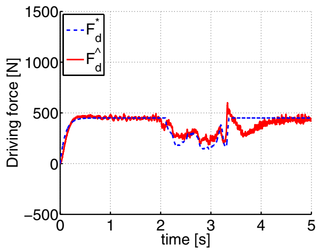

(a) Driving force.

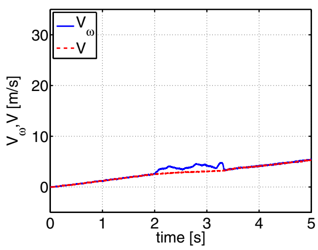

(b) Wheel velocity, Vehicle velocity.

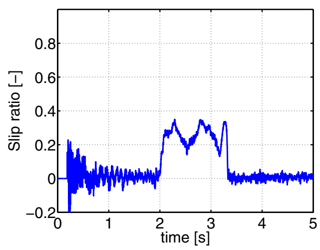

(c) Slip ratio.

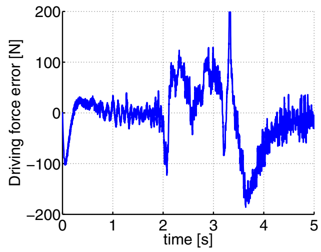

(d) Error of driving force.

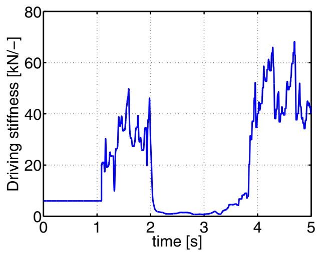

(e) Driving stiffness.

Fig. 11. Experimental Result (Proposed method 2).

[12] L. Ljung: "System Identification theory for the user", PRENTICE HALL, 1999